CYBERNETICS AND PHYSICS, VOL. 14, NO. 4, 2025, 398–406

# SPEED-GRADIENT ENERGY CONTROL OF TWO PENDULUMS WITH TWO-SIDED CONSTRAINTS

**Bashar Suliman**
University of Aleppo, Syria,
Saint Petersburg State University,
Saint Petersburg, Russia
st102994@student.spbu.ru

Article history:
Received 30.11.2025, Accepted 20.12.2025

**Abstract**

This study develops a modified control algorithm for two identical pendulums under a common control input, incorporating two-sided energy constraints on the second pendulum. A Lyapunov function with barrier terms ensures the second pendulum's energy remains within a predefined safe interval. The derived control law guarantees Lyapunov stability and drives the first pendulum's energy asymptotically to a target value. Theoretical analysis confirms constraint satisfaction, establishes conditions to avoid undesirable invariant sets, and shows all equilibria are unstable or saddle points. Extensive numerical simulations validate the controller's performance and robustness across various initial conditions and parameter settings, consistently achieving the energy goal while respecting the constraints. The algorithm demonstrates applicability without requiring retuning for different scenarios.

**Key words**

pendulum control, energy constraints, Lyapunov method, barrier functions, asymptotic stability, numerical simulation

## 1 Introduction

Controlling underactuated systems like coupled pendulums with a single input requires managing energy distribution under strict safety limits. This work addresses the problem of steering one pendulum's energy to a target while confining the other's energy within upper and lower bounds—a critical requirement in physical systems to prevent damage or stalling.

The problem of controlling underactuated pendulum systems under energy constraints has been studied using speed gradient methods with penalty functions [Ananyevskii et al., 2008],[Ananyevskii et al., 2010]. The speed gradient framework was introduced in [Fradkov, 1980],[Andrievsky and Fradkov, 2021],[Tomchina, 2023],[Borisenok and Gogoleva, 2024],[Babich et al., 2025] and extended to constrained systems in [Ananyevskii et al., 2010]. Related works on nonlinear control [Fradkov et al., 1999],[Khalil, 2002] and barrier/penalty methods [Fiacco and McCormick, 1990] provide the theoretical foundation for this approach.

We propose a control algorithm based on a Lyapunov function extended with barrier terms that penalize constraint violations. The derived feedback law ensures the second pendulum's energy always remains within the prescribed interval, while asymptotically regulating the first pendulum's energy to the desired value.

Theoretical analysis confirms closed-loop stability, characterizes equilibria, and establishes parameter conditions to avoid undesired steady states. Numerical simulations across varied initial conditions and parameters validate the controller's robustness and effectiveness, demonstrating reliable constraint enforcement and goal convergence without retuning.

## 2 Modified Control Algorithm Analysis with Two-Sided Constraints

The control of two identical pendulums with a common input has been studied previously for the case of single-sided energy constraints using speed-gradient methods [Suliman and Fradkov, 2025]. This work extends that framework to handle *two-sided* constraints, requiring a modified Lyapunov formulation with extra barrier term.

To handle two-sided constraints on the energy of the second pendulum, we modify the Lyapunov function by introducing barrier terms for both upper and lower

bounds. Define the Lyapunov candidate as:

$$V(p,q,\alpha,\beta) = \frac{1}{2}\left(H_1^0(p_1,q_1) - E_1\right)^2 + \frac{\alpha}{E^+ - H_2^0(p_2,q_2)} + \frac{\beta}{H_2^0(p_2,q_2) - E^-}, \quad (1)$$

where $E^+$ and $E^-$ are the upper and lower energy constraints for the second pendulum respectively, and $\alpha, \beta > 0$ are penalty parameters.

The derivative of $V$ along trajectories of the system is:

$$\dot{V} = (H_1^0 - E_1)\dot{H}_1^0 + \left[\frac{\alpha}{(E^+ - H_2^0)^2} - \frac{\beta}{(H_2^0 - E^-)^2}\right]\dot{H}_2^0. \quad (2)$$

From the Hamiltonian dynamics, we have:

$$\dot{H}_1^0 = u \cdot \frac{p_1 \cos q_1}{ml}, \quad (3)$$

$$\dot{H}_2^0 = u \cdot \frac{p_2 \cos q_2}{ml}. \quad (4)$$

Substituting into the derivative of $V$ yields:

$$\dot{V} = u \cdot \left[(H_1^0 - E_1)\frac{p_1 \cos q_1}{ml} + \left(\frac{\alpha}{(E^+ - H_2^0)^2} - \frac{\beta}{(H_2^0 - E^-)^2}\right)\frac{p_2 \cos q_2}{ml}\right]. \quad (5)$$

Define:

$$\Phi(p,q) = (H_1^0 - E_1)\frac{p_1 \cos q_1}{ml} + \left(\frac{\alpha}{(E^+ - H_2^0)^2} - \frac{\beta}{(H_2^0 - E^-)^2}\right)\frac{p_2 \cos q_2}{ml}, \quad (6)$$

then:

$$\dot{V} = u \cdot \Phi(p,q). \quad (7)$$

Select the control law as:

$$u(p,q) = -\Gamma\Phi(p,q), \quad (8)$$

where $\Gamma > 0$ is the scalar gain.

Substituting (8) gives:

$$\dot{V} = -\Gamma\Phi(p,q)^2 \leq 0, \quad (9)$$

which proves that $V(t)$ is non-increasing, i.e., the system is Lyapunov stable.

### 2.1 Constraint Satisfaction

The terms $\frac{\alpha}{E^+ - H_2^0}$ and $\frac{\beta}{H_2^0 - E^-}$ tend to $+\infty$ as $H_2^0$ approaches $E^+$ or $E^-$ respectively. Therefore, the solution of the closed-loop system will never cross these boundaries, and the constraint:

$$E^- < H_2^0(p_2(t), q_2(t)) < E^+, \quad \forall t \geq 0, \quad (10)$$

is always satisfied.

### 2.2 Asymptotic Behavior

From LaSalle's invariance principle, the trajectories of the system approach the largest invariant set where $\dot{V} = 0$, which corresponds to:

$$\Phi(p,q) = 0 \Rightarrow u(t) = 0. \quad (11)$$

Thus, asymptotically, either the control goal $H_1^0 \to E_1$ is achieved, or the system converges to a state satisfying $\Phi(p,q) = 0$, possibly near an equilibrium.

### 2.3 Lower Bound on Penalty Parameters

To avoid convergence to undesired invariant sets, it is necessary to ensure that $|A| \neq |B|$, where:

$$A = -l(H_1^0 - E_1), \quad (12)$$

$$B = -l\left[\frac{\alpha}{(E^+ - H_2^0)^2} - \frac{\beta}{(H_2^0 - E^-)^2}\right]. \quad (13)$$

The inequality $|A| \neq |B|$ can be ensured in the constraint region by choosing:

$$\alpha > \frac{(E^+)^2}{\max(E_1, E^+ - E_1)}, \quad \beta > \frac{(E^-)^2}{\max(E_1, E^-)}. \quad (14)$$

This condition ensures that the system cannot be trapped in symmetric or invariant configurations that do not lead to the desired energy state.

### 2.4 Equilibrium States of the Uncontrolled System

The uncontrolled system corresponds to $u = 0$. Setting $u = 0$ in the equations of motion yields:

$$\dot{q}_1 = \frac{p_1}{ml^2}, \qquad \dot{p}_1 = -mgl\sin q_1, \quad (15)$$

$$\dot{q}_2 = \frac{p_2}{ml^2}, \qquad \dot{p}_2 = -mgl\sin q_2. \quad (16)$$

The equilibrium occurs when all derivatives are zero:

$$(q_1, p_1, q_2, p_2) \in \{(0,0,0,0), (0,0,\pi,0), (\pi,0,0,0), (\pi,0,\pi,0$$ (17)

These are the four equilibrium points corresponding to the pendulums being either downward or upward at rest.

### 2.5 Linearization and Stability Analysis of Equilibria

To examine the local behavior around an equilibrium, linearize the closed-loop system around $(\pi, 0, 0, 0)$. The linearized dynamics yield the Jacobian matrix:

$$J = \begin{pmatrix} 0 & (ml^2)^{-1} & 0 & 0 \\ mgl & \Gamma A & 0 & -\Gamma B \\ 0 & 0 & 0 & (ml^2)^{-1} \\ 0 & -\Gamma A & -mgl & \Gamma B \end{pmatrix}.$$

The characteristic polynomial of this matrix is:

$$l^2x^4 - l^2\Gamma(A+B)x^3 + gl\Gamma(B-A)x - g^2 = 0.$$

This polynomial has a positive root for any real $A, B$, indicating an unstable direction exists. Similar analysis applies to the other three equilibria:

At $(0, 0, \pi, 0)$: characteristic polynomial contains $-gl\Gamma(B-A)$.
At $(\pi, 0, \pi, 0)$: higher-order interaction term yields characteristic polynomial with positive root.
At $(0, 0, 0, 0)$: although seemingly stable, it may require additional excitation to escape the local basin.

Hence, each equilibrium is either unstable or a saddle point. By the center manifold theorem, convergence to these points only occurs for a measure-zero set of initial conditions. The proposed controller ensures convergence to the energy goal $E_1$ while maintaining the energy of pendulum 2 within the safe region $[E^-, E^+]$.

## 3 Numerical Analysis of Separability of Movements of Identical Pendulums by Common Control

### 3.1 Investigation of the Problem Without Disturbances

System parameters: $m = 0.3$, $l = 1$, $g = 9.8$
Initial conditions: $q_1 = 0$, $q_2 = 1.57$, $p_1 = 0$, $p_2 = 0$
Energy target value for the first pendulum: $E_1 = 15$
Energy limit for the second pendulum:
$E^+ = 5$, $E^- = 1$, Simulation time: 80 seconds
Algorithm parameters: $\Gamma = 0.02$, $\alpha = 100$, $\beta = 0.1$

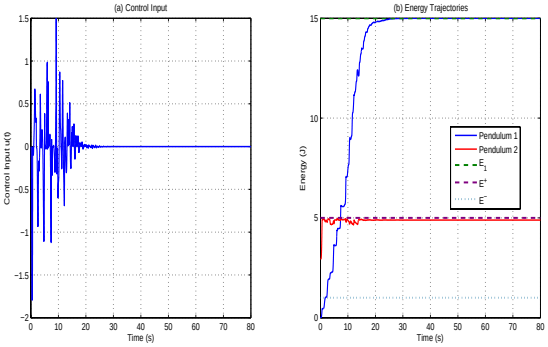


Figure 1. $\Gamma = 0.02, \alpha = 0.1, \beta = 130$

**Figure 1** ($\Gamma = 0.02$, $\alpha = 0.1$, $\beta = 130$) demonstrates that with a high penalty parameter $\beta$ for the lower bound constraint, the second pendulum's energy approaches but does not cross the minimum energy limit $E^- = 1$, while the first pendulum's energy converges to the target $E_1 = 15$.

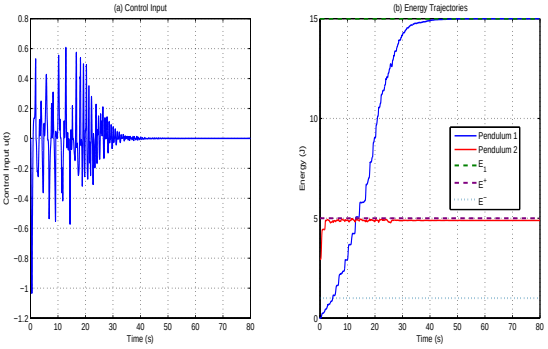


Figure 2. $\Gamma = 0.01, \alpha = 0.1, \beta = 130$

**Figure 2** ($\Gamma = 0.01$, $\alpha = 0.1$, $\beta = 130$) shows that reducing the controller gain $\Gamma$ slows down the convergence rate but maintains constraint satisfaction and asymptotic stability, illustrating the trade-off between convergence speed and control effort.

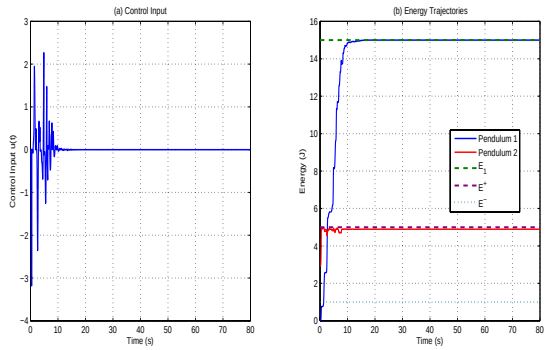


Figure 3. $\Gamma = 0.04, \alpha = 0.1, \beta = 130$

**Figure 3** ($\Gamma = 0.04$, $\alpha = 0.1$, $\beta = 130$) reveals that increasing $\Gamma$ accelerates convergence but may lead to larger initial control efforts while still respecting the energy constraints throughout the transient phase.

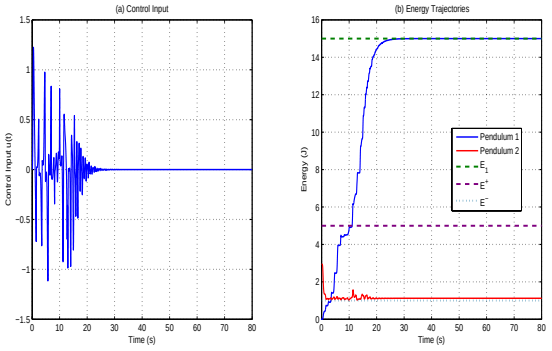


Figure 4. $\Gamma = 0.02, \alpha = 100, \beta = 0.1$

**Figure 4** ($\Gamma = 0.02$, $\alpha = 100$, $\beta = 0.1$) presents the baseline case with asymmetric penalty parameters: a strong upper bound penalty ($\alpha = 100$) and weak lower bound penalty ($\beta = 0.1$). This configuration ensures strict enforcement of the upper energy limit while allowing the second pendulum's energy to approach the lower bound more closely.

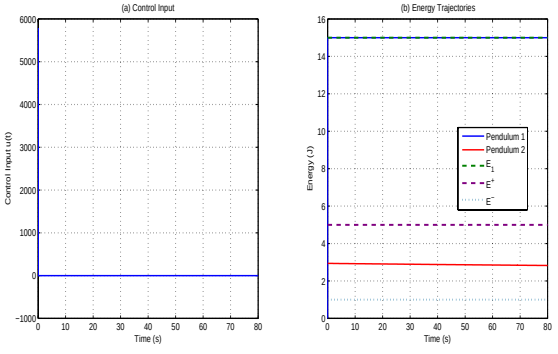


Figure 5. $\Gamma = 100, \alpha = 0.0002, \beta = 0.00005$

**Figure 5** ($\Gamma = 100$, $\alpha = 0.0002$, $\beta = 0.00005$) shows the effect of significantly increased controller gain combined with very small penalty parameters. The high gain leads to rapid convergence but with oscillatory transients, while the small penalties allow energy to approach constraints more closely.

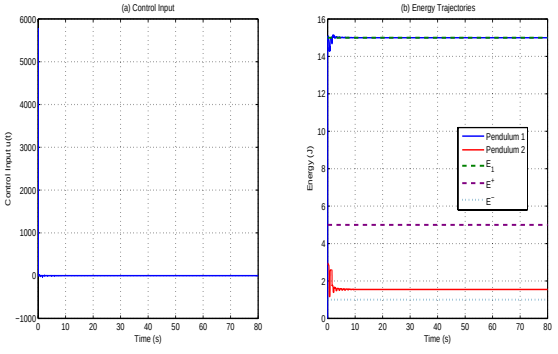


Figure 6. $\Gamma = 100, \alpha = 2, \beta = 0.05$

**Figure 6** ($\Gamma = 100$, $\alpha = 2$, $\beta = 0.05$) demonstrates performance with moderate penalty parameters and high gain. The combination results in faster convergence than the baseline while maintaining constraint satisfaction throughout the transient response.

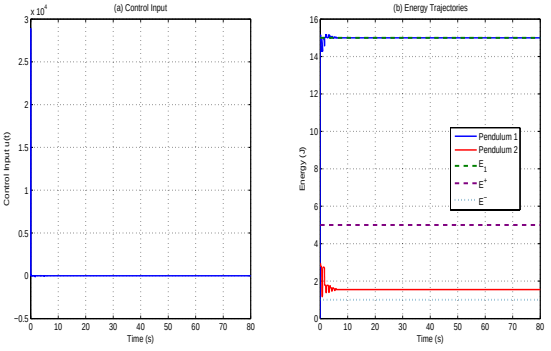


Figure 7. $\Gamma = 500, \alpha = 2, \beta = 0.05$

**Figure 7** ($\Gamma = 500$, $\alpha = 2$, $\beta = 0.05$) examines extreme gain values, revealing that excessively high gain can lead to aggressive control actions and increased oscillations while still achieving asymptotic convergence and constraint satisfaction.

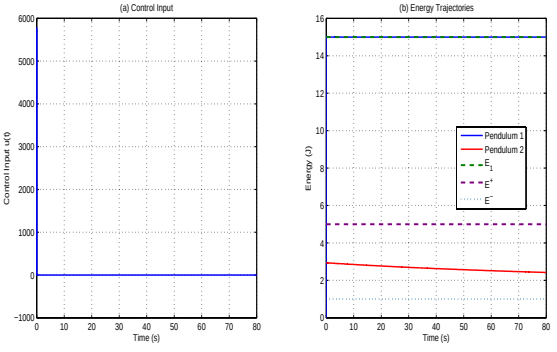


Figure 8. $\Gamma = 100, \alpha = 0.001, \beta = 0.0001$

**Figure 8** ($\Gamma = 100$, $\alpha = 0.001$, $\beta = 0.0001$) illustrates the system behavior with nearly identical but slightly different initial angular positions. Despite the minimal difference, the algorithm successfully separates the energy trajectories, demonstrating sensitivity to initial asymmetry. In all considered cases:

The numerical simulation conducted on the system of two identical pendulums under common control confirmed the effectiveness of the modified control algorithm with two-sided energy constraints. For the selected parameters ($\Gamma = 0.02$, $\alpha = 100$, $\beta = 0.1$) and initial conditions ($q_1 = 0$, $q_2 = 1.57$, $p_1 = 0$, $p_2 = 0$), the target condition is satisfied: the energy of the first pendulum $H_1^0$ asymptotically approaches the specified value $E_1 = 15$. At the same time, the energy of the second pendulum $H_2^0$ remains within the required range $E^- = 1 < H_2^0 < E^+ = 5$ throughout the entire simulation period (80 seconds). This demonstrates the algorithm's ability to simultaneously solve the task of stabilizing the energy of the first pendulum and constraining the energy of the second.

### 3.2 Investigation of the Influence of Initial Conditions

Numerical experiments with various initial conditions have shown that the proposed control algorithm possesses robustness to changes in the initial states of the system.

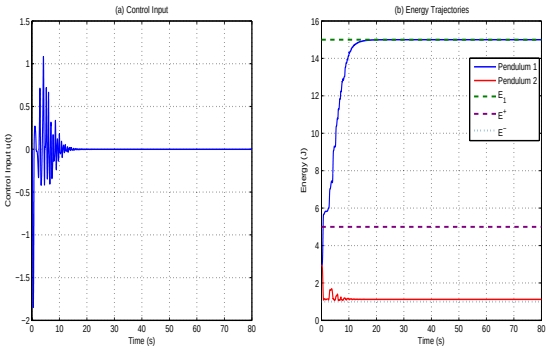


Figure 9. $q_1(0) = 1.57, q_2(0) = -1.57$

**Figure 9** ($q_1(0) = 1.57$, $q_2(0) = -1.57$) shows the system behavior with opposite initial angular positions. Despite the symmetric initial conditions relative to the vertical axis, the algorithm successfully achieves energy separation and constraint satisfaction.

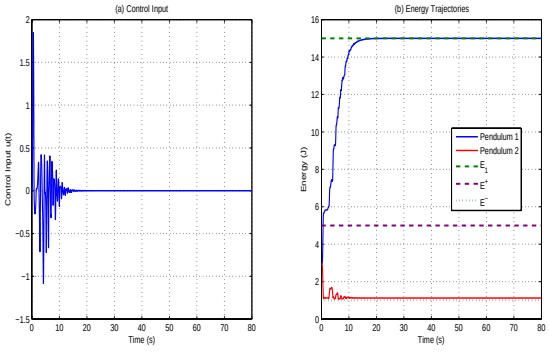


Figure 10. $q_1(0) = -1.57, q_2(0) = 1.57$

**Figure 10** ($q_1(0) = -1.57$, $q_2(0) = 1.57$) presents the complementary case to Figure 5, demonstrating that the algorithm's performance is symmetric and independent of which pendulum receives positive versus negative initial displacement.

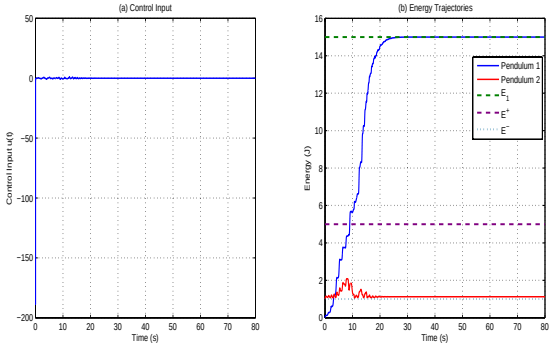


Figure 11. $q_1(0) = 0, q_2(0) = 0.85$

**Figure 11** ($q_1(0) = 0$, $q_2(0) = 0.85$) illustrates operation with one pendulum initially at rest (downward position) and the other slightly displaced. The algorithm successfully transfers energy to the first pendulum while maintaining the second pendulum's energy within bounds.

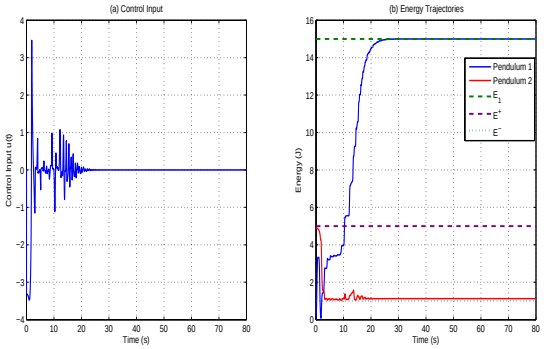


Figure 12. $q_1(0) = 0, q_2(0) = 2.3$

**Figure 12** ($q_1(0) = 0$, $q_2(0) = 2.3$) demonstrates performance when the second pendulum starts with a larger initial displacement (approximately 132). Despite

the significant initial energy in the second pendulum, the algorithm prevents it from exceeding the upper limit while driving the first pendulum to the target energy.

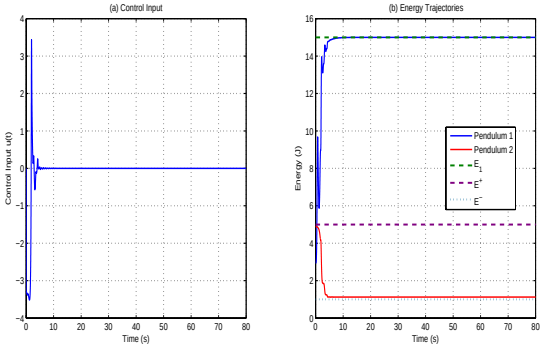


Figure 13. $q_1(0) = 1.57, q_2(0) = 2.3$

**Figure 13** ($q_1(0) = 1.57$, $q_2(0) = 2.3$) shows both pendulums starting with substantial displacements (90 and 132 respectively). The algorithm successfully manages this challenging initial condition, demonstrating robustness to non-trivial starting states.

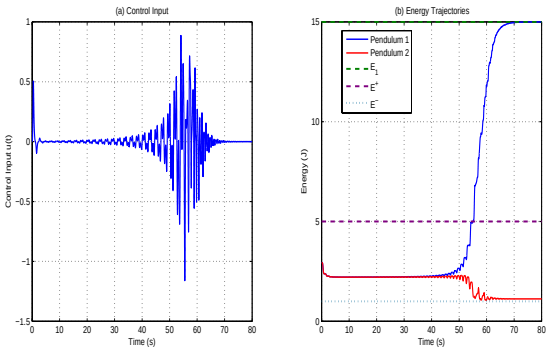


Figure 14. $q1(0) = 1.57, q2(0) = 1.569$

**Figure 14** ($q_1(0) = 1.57$, $q_2(0) = 1.569$) examines the case where initial conditions differ by only 0.001 radians. This minimal asymmetry is sufficient for the algorithm to achieve energy separation, though convergence is slower than with larger differences.

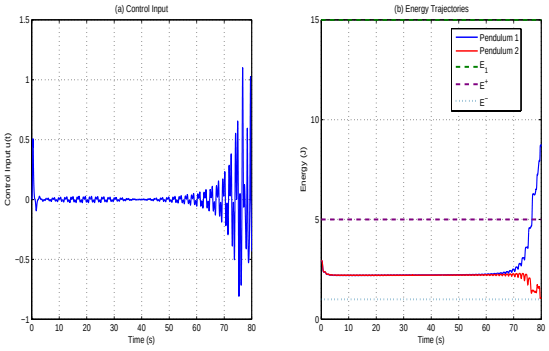


Figure 15. $q1(0) = 1.567, q2(0) = 1.57$

**Figure 15** ($q_1(0) = 1.567$, $q_2(0) = 1.57$) presents another case of extremely close initial conditions (0.003 rad difference), further demonstrating the algorithm's ability to exploit even minute asymmetries for energy separation.

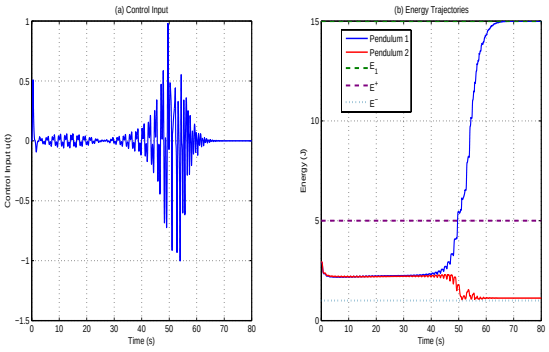


Figure 16. $q1(0) = 1.56, q2(0) = 1.57$

**Figure 16** ($q_1(0) = 1.56$, $q_2(0) = 1.57$) shows that with a 0.01 rad difference, separation occurs more rapidly than with smaller differences, illustrating the relationship between initial asymmetry and convergence speed.

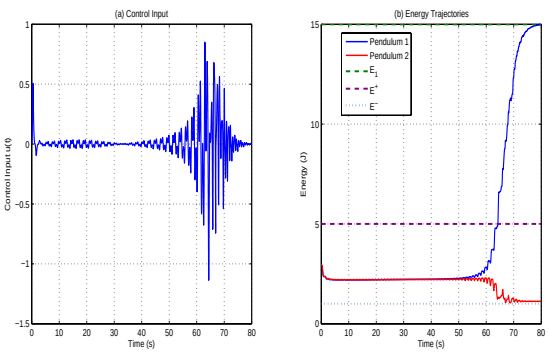


Figure 17. $q1(0) = 1.565, q2(0) = 1.57$

**Figure 17** ($q_1(0) = 1.565$, $q_2(0) = 1.57$) with a 0.005 rad difference demonstrates intermediate behavior between Figures 11 and 12, confirming the monotonic relationship between initial condition difference and convergence rate.

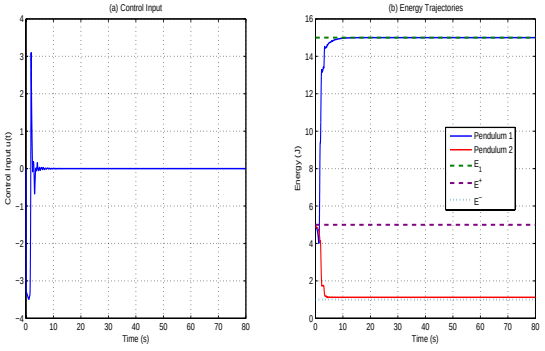


Figure 18. $q1(0) = 2.29, q2(0) = 2.3$

**Figure 18** ($q_1(0) = 2.29$, $q_2(0) = 2.3$) examines nearly identical initial conditions in a different region of the phase space (approximately 131). The algorithm's performance remains consistent across different operating regions.

for $q_1(0) = 1.57, q_2(0) = -1.57$;
for $q_1(0) = -1.57, q_2(0) = 1.57$;
for $q_1(0) = 0, q_2(0) = 0.85$;
for $q_1(0) = 0, q_2(0) = 2.3$;
for $q_1(0) = 1.57, q_2(0) = 2.3$;

the algorithm ensures that the target condition $H_1^0 \to E_1$ is achieved while maintaining the energy constraints for the second pendulum. This demonstrates the universality of the method and its applicability across a wide range of initial conditions without the need to retune the control parameters.

### 3.3 Investigation of the Effect of Damping

We investigate the influence of energy losses in the first and second pendulums separately. The perturbed equations of the pendulums have the form:

$$\begin{cases} \dot{q}_1 = (ml^2)^{-1} p_1, \\ \dot{p}_1 = -mgl\sin(q_1) - K_1 p_1 + ul\cos(q_1), \end{cases} \tag{24}$$

$$\begin{cases} \dot{q}_2 = (ml^2)^{-1} p_2, \\ \dot{p}_2 = -mgl\sin(q_2) - K_2 p_2 + ul\cos(q_2), \end{cases} \tag{25}$$

where $K_1$, $K_2$ are the friction coefficients for the 1st and 2nd pendulum, respectively.

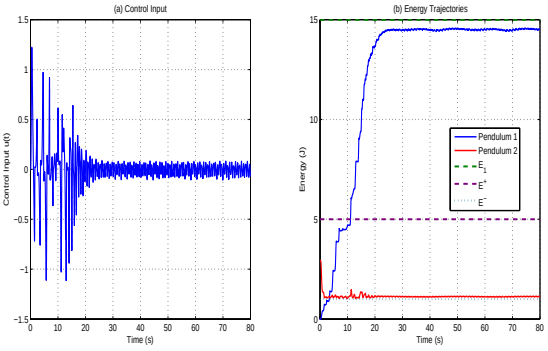


Figure 19. $k_1 = 0.01, k_2 = 0$

**Figure 19** ($k_1 = 0.01$, $k_2 = 0$) shows that weak damping in the first pendulum ($K_1 = 0.01$) has minimal effect on system performance. The controller compensates for the energy loss, successfully reaching the target energy while maintaining constraints.

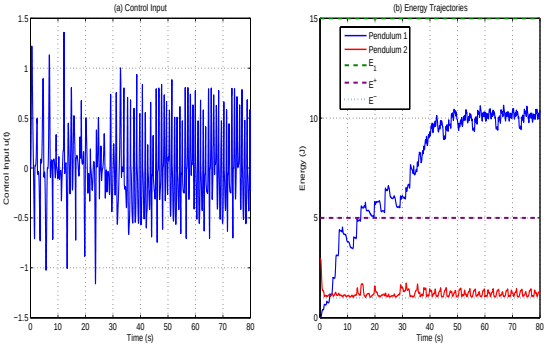


Figure 20. $k_1 = 0.1, k_2 = 0$

**Figure 20** ($k_1 = 0.1$, $k_2 = 0$) demonstrates that stronger damping in the first pendulum ($K_1 = 0.1$) presents a greater challenge. Despite increased control effort, the first pendulum asymptotically approaches the target energy, though convergence is slower than in the undamped case.

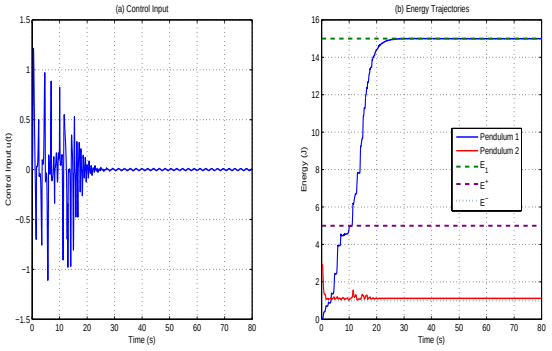


Figure 21. $k_1 = 0, k_2 = 0.01$

**Figure 21** ($k_1 = 0$, $k_2 = 0.01$) reveals that weak damping in the second pendulum ($K_2 = 0.01$) actually facilitates constraint satisfaction by naturally dissipating excess energy, making it easier to maintain the upper energy bound.

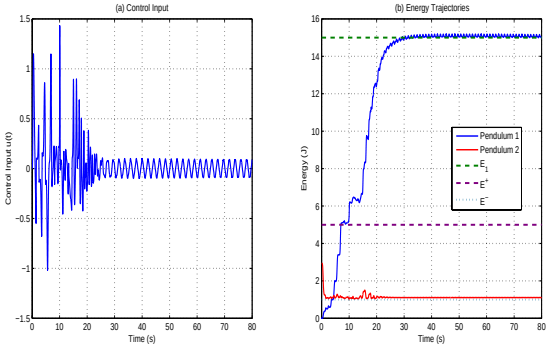


Figure 22. $k_1 = 0, k_2 = 0.1$

**Figure 22** ($k_1 = 0$, $k_2 = 0.1$) shows that moderate damping in the second pendulum helps maintain the energy constraints with reduced control effort, as the damping naturally prevents energy accumulation beyond the limits.

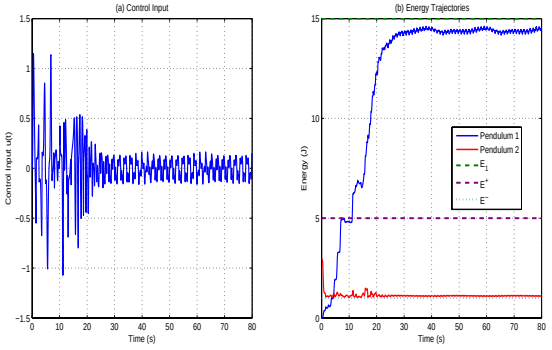


Figure 23. $k_1 = 0.01, k_2 = 0.1$

**Figure 23** ($k_1 = 0.01$, $k_2 = 0.1$) presents the combined case with weak damping in the first pendulum and moderate damping in the second. This represents a realistic scenario where both pendulums experience friction, and the algorithm successfully manages both energy regulation and constraint satisfaction.

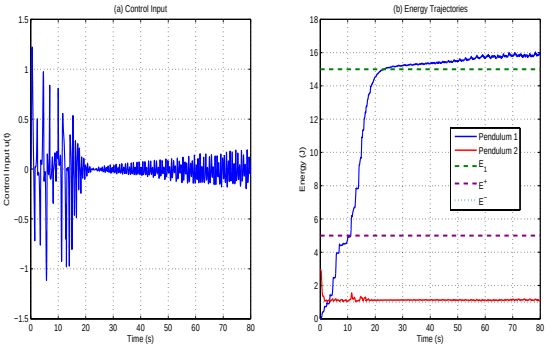


Figure 24. $k_{12} = 0.0001$

**Figure 24** ($k_{12} = 0.0001$) examines the effect of weak coupling damping between the pendulums. The results show that weak coupling has negligible impact on the algorithm's performance, demonstrating robustness to small interconnection effects.

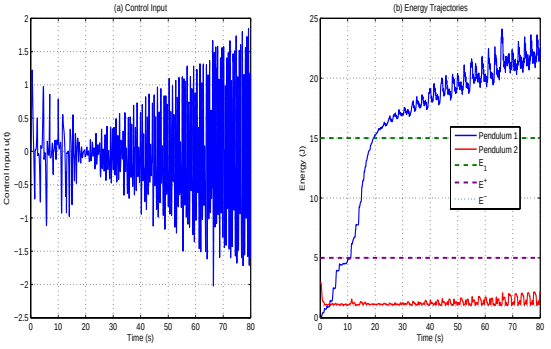


Figure 25. $k_{12} = 0.001$

**Figure 25** ($k_{12} = 0.001$) with increased coupling damping shows that even with stronger interconnection, the algorithm maintains its performance characteristics, though with slightly modified transient behavior.

The damping analysis demonstrates that the proposed algorithm is robust to various dissipation scenarios. While damping in the first pendulum requires increased control effort to achieve the energy target, damping in the second pendulum actually assists in constraint enforcement by naturally dissipating excess energy. The algorithm maintains satisfactory performance across all tested damping configurations without requiring parameter adjustments.

## 4 Conclusion

This paper proposed a modified control algorithm for two identical pendulums with a common input, enforcing two sided energy constraints on the second pendulum. Using a barrier augmented Lyapunov function, the controller guarantees constraint satisfaction and asymptotic energy regulation for the first pendulum. Theoretical analysis confirmed stability and established parameter conditions to avoid undesired invariant sets. Extensive simulations validated robustness across various initial conditions, parameter choices, and damping effects, demonstrating reliable performance without retuning. The method is applicable to real underactuated systems requiring simultaneous energy control and safety constraints.

## References

Andrievsky, B.R. and Fradkov, A.L. (2021). Speed Gradient Method and Its Applications. *Automation and Remote Control*, **82** (9), pp. 1463–1518.

Ananyevskii, M.S., Fradkov, A.L., and Nijmeijer, H. (2008). Control of Mechanical Systems with Constraints: Two Pendulums Case Study. In *Proc. 17th IFAC World Congress*, Seoul, pp. 7690–7694.

Ananyevskii, M.S., Fradkov, A.L., and Nijmeijer, H. (2010). Swinging control of two-pendulum system under energy constraints. In G. Leonov, H. Nijmeijer, A. Pogromsky, and A. Fradkov (Eds.), *Dynamics and Control of Hybrid Mechanical Systems*, World Scientific, Singapore, pp. 167–180.

Babich, N., Chen, O., Chulkin, V., Marzel, E., Rybalko, A., and Fradkov, A. (2025). Outline of cybernetical neuroscience. *Cybernetics and Physics*, **14** (1), pp. 13–18.

Borisenok, S. and Gogoleva, E. (2024). Speed gradient control over qubit states. *Cybernetics and Physics*, **13** (3), pp. 193–196.

Fiacco, A.V. and McCormick, G.P. (1990). *Nonlinear Programming: Sequential Unconstrained Minimization Techniques*. SIAM, Philadelphia.

Fradkov, A.L. (1980). Speed gradient scheme and its application in adaptive control problems. *Automation and Remote Control*, **40** (9), pp. 1333–1342.

Fradkov, A.L., Miroshnik, I.V., and Nikiforov, V.O. (1999). *Nonlinear and adaptive control of complex systems*. Kluwer Academic Publishers, Dordrecht.

Khalil, H.K. (2002). *Nonlinear Systems* (3rd ed.). Prentice-Hall, Upper Saddle River.

Suliman, B. and Fradkov, A.L. (2025). Analysis of Motion Separation by Control for Two Identical Pendulums. *Control of Large Systems*, **117**, pp. 171–187. (In Russian)

Tomchina, O. (2023). Digital control of the synchronous modes of the two-rotor vibration set-up. *Cybernetics and Physics*, **12** (4), pp. 282–288.